Virus Research 368 (2026) 199741

Contents lists available at ScienceDirect

Virus Research

journal homepage: www.elsevier.com/locate/virusres

A mycovirus-encoded homologue of plant viral movement proteins is not functional in movement complementation assays in plants

Federica Bono [a,1], Ian Martinelli [a,1], Yi Guo [b], Saul Pagnoni [c], Frederic Aparicio Herrero [d], Massimo Turina [b,e,*]

[a] Department of Molecular and Translational Medicine, University of Brescia, Via Branze 39, 25123, Brescia, Italy
[b] Institute for Sustainable Plant Protection, National Research Council of Italy, Strada delle Cacce 73, 10135 Torino, Italy
[c] Department of Agricultural and Environmental Sciences - Production, Landscape, Agroenergy, University of Milan, via Celoria 2, Milan 20133, Italy
[d] Institute for Plant Molecular and Cellular Biology (IBMCP, UPV-CSIC) Av Fausto Elio s/n, 42022 Valencia, Spain
[e] Department of Plant Protection, School of Agriculture, The University of Jordan, Amman, 11942, Jordan

ARTICLE INFO

Keywords:
Mycovirus
Movement proteins
Coguvirus
Bocivirus
Cross-kingdom infections

ABSTRACT

Valsa mali negative strand RNA virus 1 (VmNSRV1), a fungal virus infecting *Valsa mali* and belonging to the *Phenuiviridae* family, was recently shown to be capable of naturally infecting plants. Its RNA2 encodes a homologue of a plant virus movement protein (MP) that can complement MP-deficient virus vectors and localizes to plasmodesmata, allowing natural cross-kingdom infection. To determine whether this property is a common feature among mycoviruses possessing distant MP homologues or an isolate-specific trait, we investigated Trichoderma gamsii cogu-like virus 1 (TgClV1), a *Phenuiviridae* member in the *Bocivirus* genus detected in *Trichoderma gamsii*. Structural analysis guided by AlphaFold confirmed that the RNA2-encoded open reading frame (ORF) contains a conserved seven beta-strand module characteristic of the 30 kDa MP superfamily, making it a putative MP-like protein (MP-L). To assess its functional role, we tested whether TgClV1's putative MP (TgCl-MPl) could complement movement-deficient plant viruses, employing tomato apex necrosis virus (ToANV), alfalfa mosaic virus (AMV), and potato virus X (PVX) MP-deficient vectors. While tobacco mosaic virus-MP successfully complemented cell-to-cell movement in trans in all these systems, TgCl-MPl did not. Additionally, localization studies of TgClV1-MPl-GFP fusions revealed that, unlike TMV-MP and VmNSRV1-MP, TgClV1-MPl did not specifically target plasmodesmata, a key characteristic of functional viral MPs. Finally, direct inoculation of *Nicotiana benthamiana*—either via mechanical application of purified TgClV1 or via natural inoculation through TgClV1-infected *Trichoderma gamsii* associated with plant roots—failed to establish infection. In conclusion, our findings do not support the hypothesis that TgClV1-MPl functions as a plant virus movement protein. The evolutionary implications of this observation are discussed.

1. Introduction

The untargeted search for viruses through specific bioinformatic pipelines applied to high throughput sequencing (HTS) data both from meta-transcriptomes and metagenomes has increased exponentially the description of the biodiversity of *bona fidae* viruses or of subcellular RNA infectious elements. These studies initially pointed to invertebrates (particularly arthropods) as the main hub for viral diversification (Shi et al., 2016), but more recently studies of fungal- and oomycete-based viromes (Forgia et al., 2024) have also greatly enriched viral biodiversity, pointing to fungi and fungal-like organisms as an additional hub for plant viral diversification and spread. In this respect viruses infecting fungi and protists with a fungal lifestyle are commonly named mycoviruses even if those infecting protists have a specific set of viruses and recently the name ooviruses has been proposed for them.

The large datasets used for phylogenetic analyses pointed to cross-kingdom host adaptation events developing over long evolutionary times particularly between fungi and plants: fungi establish with plants a range of symbiotic relationships, that bring fungal and plant cells in close contact and constant dialogue, with potential for cross-kingdom

* Corresponding author.
E-mail address: massimo.turina@cnr.it (M. Turina).
[1] Federica Bono e Ian Martinelli contributed equally to this work.

https://doi.org/10.1016/j.virusres.2026.199741
Received 28 February 2026; Received in revised form 27 April 2026; Accepted 1 May 2026
Available online 1 May 2026

reciprocal adaptations.

One of the first evidence of possible horizontal inter-kingdom transfer between mycovirus and plants came from the early discovery that some closely related *bona fidae* plant viruses and mycoviruses were included in the same taxonomic viral family or in some cases even genus: such is the case, of members of the families *Endornaviridae, Chrysoviridae, Partitiviridae, Totiviridae*, and *Mitoviridae* (Nerva et al., 2019; Takahashi et al., 2019) . Such plant viruses, however, have the distinctive feature of being able to infect plant cells but are unable to move cell-to-cell through plasmodesmata (PD) and therefore cannot be transmitted mechanically; they can maintain persistent infection in the plants because they have the unusual capacity to infect meristematic tissues and embryos, and therefore are very well transmitted vertically through seeds. Although they are *bona fidae* plant viruses, they all lack the hallmark of plant viruses, which is one (or more) virus-encoded proteins that facilitate the passage of viral RNA or whole particles to neighbouring cells through PD: such proteins are functionally defined as movement proteins (MP). Viral MPs are polyphyletic, but the most abundant family is the 30 kDa family of MPs which is structurally conserved (Dorokhov et al., 2020). The tobacco mosaic virus MP (TMV MP) is the best studied among viral MPs, and some functional domains have been characterized: these include RNA and ATP binding, and cell wall targeting regions (Heinlein, 2015a; Heinlein, 2015b).

Since the early discovery of plant-fungal-virus promiscuous taxonomic clades a number of experimental systems have shown that often plant cells and fungal cells share the basic genetic makeup to support cell autonomous viral replication: fungal cells (yeast) have been shown to support replication of plant viruses (Janda and Ahlquist, 1993) and plant cells were shown to support mycovirus replication (Nerva et al., 2017). Later fungi were shown to naturally harbour plant virus infections (Andika et al., 2017).

More recently, some confirmed mycoviruses (maintained in axenically grown fungal colonies) were shown to encode proteins homologous to plant movement proteins. The first such example was revealed in Botrytis cinerea cogu-like virus (Ruiz-Padilla et al., 2021), but later it was shown that such conservation is also present in other phenuivirids both from metatrascriptomic samples, and from taxonomic clades including both plant and fungal viruses. Among them is a virus infecting *Trichoderma gamsii* isolated from Sardinia (Pagnoni et al., 2023): the virus Trichoderma gamsii cogu-like virus 1 (TgClV1) belongs to the same recently established genus *Bocivirus* in the *Phenuiviridae* in the order *Hareavirales* in the class *Bunyaviricetes* (Kuhn et al., 2024; Sasaya et al., 2023). The tri-segmented genome of the virus codes for an RNA dependent RNA polymerases in the larger segment, for a putative nucleocapsid in the smaller segment, and for a protein of unknown function encoded by the middle segment with distant similarity to other putative plant virus MP present in other plant-infecting viruses in the same family *Phenuiviridae,* specifically those belonging to the recently established genus *Coguvirus* (Navarro et al., 2018).

One member of this family, Valsa mali negative strand RNA Virus 1 (VmNSRV1), was recently shown to be naturally able to infect both *Valsa mali*, the fungal host where it was originally identified, and *Malus domestica* and *Nicotiana benthamiana*, a natural plant host and a laboratory plant host respectively (Dai et al., 2024).

The purpose of this study is to compare protein structures and derive in silico predictions of the structure of the TgClV1-encoded putative movement-like protein (from here on, TgClV1-MPl) and verify if this protein is functionally a movement protein through complementation assays using movement-deficient plant virus infectious clones. The implications of the results obtained will be discussed in the context of the recent identification of the putative origin of the conserved domain detected in 30kDa plant viral MP (Butkovic et al., 2023).

2. Materials and methods

2.1. In silico analysis (alignment and structural)

We used the TgClV1-MPl protein as query to search for homologues in protein databases by BLASTp using default settings. Among the hits, we selected several MP from verified plant viruses and a number of bona-fidae coguviruses (likely plant viruses, but with no real in vivo experimental validation of their MP) and cogu-like viruses, some of which of certain fungal origin, because they are present in fungi grown axenically on artificial substrate for many passages.

Putative MP-like proteins from different taxonomic groups were aligned using both the online version of Clustal Omega software (Sievers et al., 2011) and the MAFFT (Katoh et al., 2019) alignment algorithm, with default settings, at the EBI Web Services (Madeira et al., 2024). PROMALS3D was also used for multiple alignment with evolutionary and three-dimensional structural information (Pei and Grishin, 2014).

Subsequent alignment results were first screened using MEGA 12 software (Kumar et al., 2024) to evaluate the proper alignment of D residue in the putative conserved 30kd subdomain (see results). Then the same alignment results were submitted to the IQ-TREE web server (Lam-Tung et al., 2015) to produce phylogenetic trees under maximum-likelihood model (Trifinopoulos et al., 2016), with the best substitution model estimated automatically by IQ-TREE with Model Finder (Kalyaanamoorthy et al., 2017) and ultrafast bootstrap analysis in which 1000 replicates were performed (Diep Thi et al., 2018). The specific model for each tree is indicated in the figure caption in the results section.

Protein 3D structure was predicted in-silico using Alphaphold3 (Abramson et al., 2024). Models obtained were then employed for structural comparison and Root Mean Square Deviation (RMSD) estimation using UCSF ChimeraX 'matchmaking' function, with default parameters. ChimeraX was used to display graphically the structures (Pettersen et al., 2021). Protein 3D structure database searches were performed using FoldSeek (van Kempen et al., 2024) searching the PDB100 20240101 and BFVD 2023_02 (Kim et al., 2024).

2.2. Cloning of MP and MPl coding sequence in vectors for transient expression in plants

A Trichoderma gamsii cogu-like virus 1 (TgClV1)-infected fungal isolate for amplifying the TgCl-MPl was provided from a collection of isolates from Sardinia previously described (Migheli et al., 2009). The virus was detected in the isolate 22-26, renumbered "33" in a previous work (Pagnoni et al., 2023). The tobacco mosaic virus isolate used in this study was Ta9 from tobacco from Veneto Region (Italy) mantained in the PLAVIT collection.

The lyophilized mycelia stored in Eppendorf tubes were first disrupted by bead-beating (FastPrep-24 MP Biomedicals); the resulting powders were then employed for total RNA extraction with "Spectrum Plant Total RNA" kit (Sigma-Aldrich) as previously detailed (Chiapello et al., 2021).

RNA concentration was inferred from UV absorbance at 260 nm and 260/280 ratio evaluation was used as a quality indicator: both measures were obtained using a NANODROP LITE Spectrophotometer (Thermo Fisher Scientific).

To amplify cDNA fragments, we choose for reverse transcription reaction Superscript® IV Reverse Transcriptase (Invitrogen) using both random primers and a specific primer as trigger; the reaction developed at 55°C following exactly the producer's provided protocol.

Viral cDNA was amplified starting from total cDNA using different primer pairs spanning from a few nucleotides upstream of the TgClMPl AUG until the stop codon (included); the primers also included the *Stu*I restriction site sequence (for the forward primer) and the *Not*I restriction site sequence for the reverse primers. Sequence of each primer is detailed in Supplementary online Table 1.

For the PCR reactions "Phusion High-Fidelity PCR Kit" (New England BioLabs) was used, in the following conditions: 10µl buffer5X, 5µl dNTPs 2mM, 2,5µl forward primer 10µM, 2,5µl reverse primer 10µM, 1µl cDNA, 30µl H2O and 0,4µl Phusion polymerase (2U/µl). Life Pro Thermal Cycler (Bioer Serves Lifes) thermocycler was set at 98°C for 3', then for 35 cycles each composed by 20" at 98°C, 20" at 58° and 15" at 72°C. 5µl of PCR products were run in a 1% agarose TAE (40mM Tris, 20mM acetic acid, 1mM EDTA) electrophoresis stained with SYBR Safe Gel Stain run for 30' at 120V; at the end of the run the gel was examined at the UV transilluminator to select the samples with bands of the expected length. The remaining 45µl of PCR products were run in a new agarose electrophoresis run to purify the bands with the length of interest from the gel. Purification was achieved with the help of a scalpel and then using Zymoclean Gel DNA Recovery Kit (ZymoResearch), following the producer's provided protocol. Purified DNA fragments were cloned in the pCR-Blunt vector provided with Zero Blunt PCR Cloning Kit (Invitrogen); for ligation reaction we slightly adjusted company's provided protocol to our lab conditions: in a tube were added, in order, 4µl PCR product, 2µl buffer5X, 2,25µl H2O, 0,75µl pCR-Blunt vector and 1µl Express Link T4 DNA ligase (5,0 WeissU/µl); the reaction was carried out for 1h at RT.

For the transformation we used DH5α competent cells which were prepared following the instructions of the "Z-Competent E. coli" (ZymoResearch) kit.

After checking all the sequences of the clones inside topo blunt vector by Sanger sequencing with M13F and M13 Rev primer (BioFab Research, Rome, Italy), all the clones were cut with the restriction enzyme *Stu*I and *Not*I (Enza, Invitrogen).

Additionally, pJL22 binary expression vector that hosts inserts downstream of a double 35S promoter (Lindbo, 2007; Liu and Kearney,

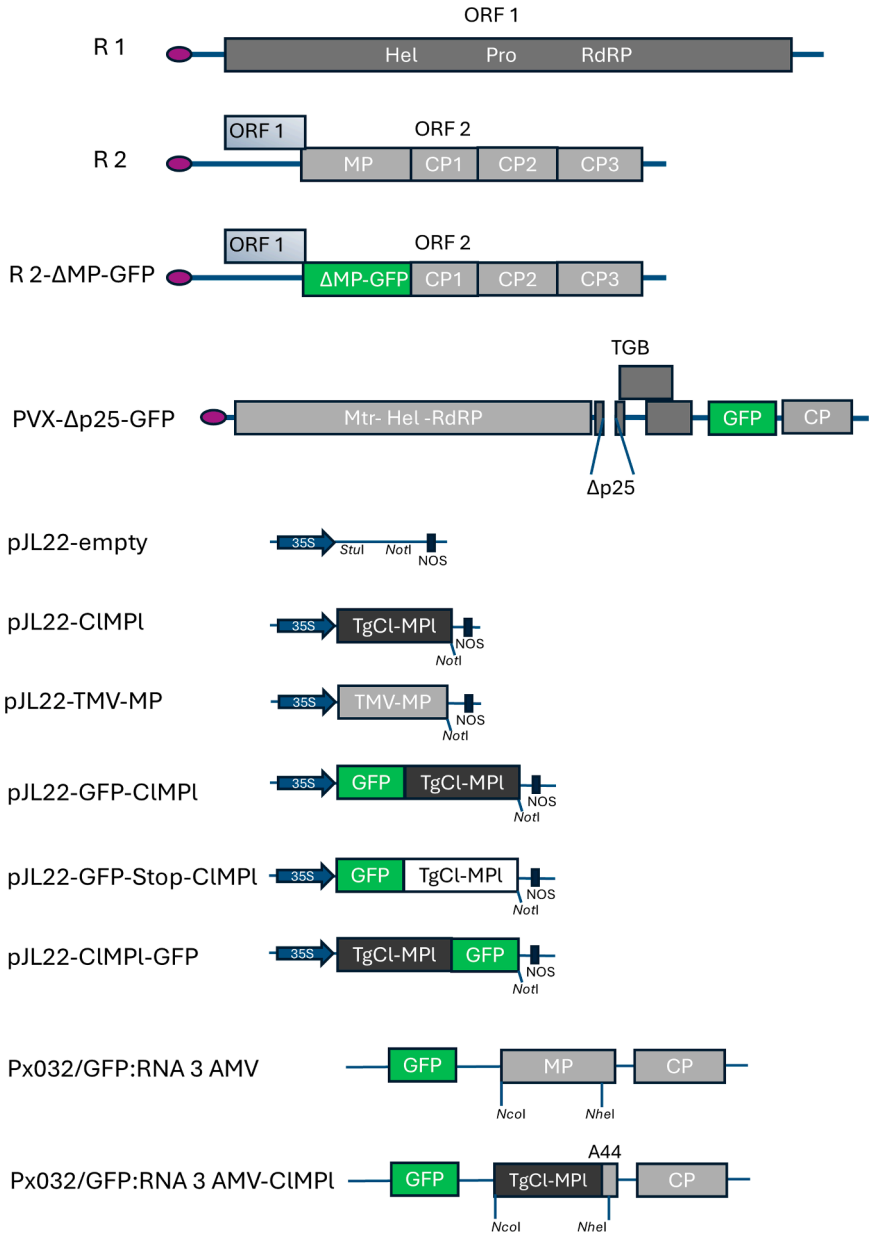

Figure 1. Graphic representation of the main clones used in this work. Tomato apex necrosis (ToANV) and potato virus X (PVX) movement protein mutants were previously described (see materials and methods section) while the rest of the constructs were prepared for this work. 35S= 35 S promoter. NOS= Nos Terminator. GFP= Green fluorescent protein. MP= movement protein. TgCl-MPl= Trichoderma gamsii Cogu-like Virus 1-MP-like protein. CP= coat protein. A44 is a fragment of AMV-MP fused at the carboxy-terminus of the ClMP-l; Hel= helicase domain; Pro=Protease domain; RdRP= RNA-dependent RNA polymerase; Mtr= Methyl transferase domain; ΔMP-GFP is a deletion of the ToANV MP fused to GFPV.

2010) was also digested with *Stu*I and *Not*I. The reaction was heat inactivated (20 min at 70°C) and the linearized vector was gel-purified for ligation.

Ligation of cut MP coding fragments and cut vector with T4 ligase (Thermo Scientific) was carried out as described above at for 2 hrs at room temperature. The pJL22-TMV-MP and pJL22-TgCl-MPl proteins expressing constructs are graphically described in Fig. 1.

The AMV system uses transgenic *Nicotiana benthamiana* plants P12 and an RNA3 vector (Sanchez-Navarro et al., 2001; Sánchez-Navarro and Bol, 2001; Sánchez-Navarro et al., 2006). The RNA 3 vector allows replacement of the MP by the insertion in frame in *Nco*I-*Nhe*I restriction sites of the desired MP. Because an *Nhe*I restriction site is present in the sequence coding for TgCl-MPl protein, we first mutagenized the plasmid by inverse PCR to eliminate the restriction site without changing the protein sequence with oligonucleotides detailed in Supplementary online Table 1. We then amplified the coding sequence with oligos that included *Nco*I and *Nhe*I sites to allow in-frame translation of the fusion with the A44 fragment from AMV MP. The TgCl-MPl coding fragment was digested and ligated in the *Nco*I- *Nhe*I sites of vector allowing fusions as detailed.

2.3. Cloning of GFP-MP-like fusion proteins in JL22 expression vector

We performed a PCR-mutagenesis on the TgClV1-MP-like coding sequence to insert a *Pac*I site at the amino terminal protein amino-terminal using the oligonucleotide described in Supplementary online Table 1 and Phusion long PCR enzyme in the conditions described above, using an extension time of 6 min. Mutagenesis was carried out on the pCR-Blunt-TgClV1-MP intermediate and then, after sequencing, transferred to pJL22 using the *Stu*I-*Not*I primers as above. We then inserted a GFP coding sequence flanked by two *Pac*I sites with two different reverse primers: in one case a stop codon is inserted, in order to avoid translation of the fusion GFP-MPl, in the other case, the reverse primer allowed an in-frame fusion so that just the entire fusion protein is potentially expressed: the two plasmids are named pJL22-GFP-ClMPl and pJL22-GFP-Stop-ClMPl respectively (Fig. 1). A C-terminal TgClV1-MPl-GFP fusion construct was also generated following the same cloning rationale (pJL22-ClMPl-GFP). Agroinfiltration of the constructs for transient expression was carried out with *Agrobacterium tumefaciens* bacterial suspensions which were mixed in equal amount with a silencing suppressor-expressing *A. tumefaciens* culture (TBSV p19). From agroinfiltrated leaves we also derived protoplasts as previously described(Margaria et al., 2015).

2.4. Complementation assays

We assayed the functional capability of complementing MP deletion mutants of viruses in three different systems, tomato apex necrosis virus (here for the first time used for this purpose), potato virus X (PVX) and alfalfa mosaic virus (AMV).

An infectious clone of tomato apex necrosis virus (Turina et al., 2007) was derived which allowed to perform specific mutagenesis and a reverse genetic approach that brought to the identification of this virus's MP protein (Ferriol et al., 2016). From the infectious clone, a specific virus vector expressing GFP with most part of the MP deleted (R2-ΔMP-GFP) was previously shown to express GFP only in the cells where it is expressed, without possibility to move from cell to cell (Ferriol et al., 2018) (Fig. 1).

To test if our TgCl-MPl protein could complement in trans the ToANV-ΔMP mutant, we agroinfiltrated bacterial culture suspensions at a saturating concentration of the MPl-expressing construct, and serial dilution (1/5) of the RNA2-deltaMP GFP vector to ensure single-cell infections (obtained at 1/625).

In detail, each agroclone was grown overnight in a 2 mL kanamycin and tetracycline (50 and 5 ug/ml) LB medium at 28°C. 0.5 mL of the o/n culture were then used to start a 20 mL solution grown overnight in 50 mL conical tubes at 28° C with the same media as above. A pellet was harvested by spinning in a Heraeus Megafuge 16R (Thermo Scientific) centrifuge (Thermo Scientific) with a swinging bucket rotor T75003181for 20 min at 4800 rpm. The pellet was resuspended in 10 mL resuspension buffer (10 mM MES pH5.5, 10 mM MgCl2 and 100 μM Acetosyringone). All the different suspensions were diluted and normalized to 0.3 OD (600 nM).

For our specific complementation experiments, *A. tumefaciens* suspensions expressing RNA1 of ToANV (necessary for RNA2 expression) and each of the three complementing suspensions expressing the test constructs (pJL22-empty, vectors pJL22-ClMPl, and pJL22-TMV-MP) were used in all the agroinfiltrations, in equal volumes of the RNA1 suspensions at the initial concentration of 0.3 O.D. This ensured that each plant cell could be delivered with the constructs (this was preliminary assessed using a GFP expressing plasmid). Instead, the RNA2 of ToANV with MP deleted and expressing GFP was agroinfiltrated in serial dilution (1:5) at least for 7 dilutions, to assess single cell inoculation. *Nicotiana benthamiana* plants were used (20 cm high, circa 50 days after sowing) for agroinfiltration experiments.

For PVX we used a viral vector expressing GFP where one of the triple gene block proteins was deleted, making the vector unable to move (Sun et al., 2013); agroinfiltration experiments were performed as described above.

The experimental setup for the AMV system uses transgenic plants P12 and an RNA3 transient expression vector were described in detail previously (Sánchez-Navarro et al., 2006).

All plants were kept in a growth chamber with 12 h daylight at 26°C using LED artificial lights (SPIDER FARMER SF600); plants were occasionally supplemented with Miracle-Gro fertilizer.

2.5. Confocal microscope observation and statistical analysis

Plant sections and protoplast suspensions were examined using a Zeiss LSM 880 confocal microscope equipped with Plan-Apochromat 20X objective (Carl Zeiss AG, Oberkochen, Germany). GFP was excited with the 488 nm line of an Argon laser and imaged through an emission window of 500–525 nm. Chlorophyll was excited with the same 488 nm Argon laser and emission was collected at 650–700 nm. Brightfield images were acquired using the ESID detector. Images were acquired and examined using the ZEN 2.3 software (Carl Zeiss AG, Oberkochen, Germany).

Complementation efficiency was quantified by counting infection foci classified as single cells, 2-3 cells, or clusters (>3 cells). Four biological replicates were analyzed per treatment. Data are presented as mean ± SEM from four biological replicates. Differences in cluster formation among treatments were assessed using the Kruskal-Wallis test, followed by pairwise Mann-Whitney U tests with Bonferroni correction for multiple comparisons (corrected $\alpha = 0.0167$). Effect sizes were calculated as $r = Z/\sqrt{N}$. Statistical significance was set at $P < 0.05$. All analyses were performed using Python 3.12 with SciPy 1.11. The subcellular localization and PVX and ToANV complementation experiments were repeated at least three times. The AMV complementation experiment was carried out once.

2.6. In vivo plant inoculation assays

Mycelium from a liquid culture (PDB) of strain 2226 was harvested using Miracloth 3 days post inoculation. Twelve grams of wet mycelia were added to 70 ml of extraction buffer (0.2 M tris pH8, 0.01 M DIECA, 0.05 M EDTA, and 0.02 M Thioglycolic Acid). Mycelia and buffer were homogenized using TissueRuptor II (Qiagen) for 5 min. Extract was separated by unbroken mycelia with a 5 min spin at 4000 RPM. The supernatant was then spun again for 10 min at 9000 RPM (Fixed angle) originating S2 (supernatant) and (P2). The supernatant was treated with Triton X 100 for 1 hr (1 %). A further 10 k spin for 10 min was carried out to generate P3 and S3. S3 was loaded on a sucrose cushion (5 ml 20%

sucrose) using Ti45 rotor for 3 hrs at 35 k RPM. Pellet (P4) was resuspended O/N.

Mechanical inoculation of *N. benthamiana* plants with partially purified virus (fraction P4 diluted 1/10 in inoculation buffer with carborundum) was performed as previously described (Turina et al., 2006). A P2 suspension was diluted 1/10 and also infiltrated in *N. benthamiana* leaves.

Tomato plants were inoculated with mycelial homogenate (1/8 of a freshly grown plate, homogenized in sterile water). Two ml of homogenate were inoculated 15 days after sowing (first true leaf) with direct placement in the soil (originally autoclaved). The inoculation was repeated 7 days after.

Roots were washed and examined by qRT-PCR using total RNA as template, extracted as specified above. A fast protocol for detection in leaves and roots (Margaria et al., 2009) was also used using primers and probe specified in Supplementary online Table 1.

The inoculation experiments were carried out twice.

3. Results

3.1. Phylogenetic analysis

The protein TgCl-MPl was initially annotated as a hypothetical protein with no function assigned. BLASTp analysis using default settings revealed numerous hits to different RNA2-encoded proteins of the members of some genera in the *Phenuiviridae*, a complex family that was initially established joining phlebovirids and tenuivirids. The family now comprises a number of newly established genera that include some viruses able to infect vertebrates and arthropods (phleboviruses), plants (tenuiviruses, coguviruses), and viruses that infect fungi (bocivirus, lentinovirus, entovirus). Some new genera in the family were derived from meta-samples, and a biological proof of the host cells is often missing (rubodvirus, laulavirus). Specifically, the hits with the highest BLAST score were proteins belonging to the genera *Bocivirus, Coguvirus, Laulavirus, Rubodvirus, Lentinovirus, Entovirus* (Supplementary online Table 2). Most of these proteins have a predicted molecular mass of approximately 50 kDa, but those of the *Laulavirus* members, including VmNSRV1, are close to 80 kDa in mass (Supplementary online Table 3).

BLASTp analysis identified as the first confirmed plant MP (but below the threshold) those of the family *Aspiviridae*, a family that is only distantly related to the *Phenuiviridae*, and it is outside the *Bunyavericetes* class, which includes the plant infecting *Tospoviridae and Fimoviridae* families along with the genus *Tenuivirus*.

As representative of the BLASTp list of hits, the proteins listed in Supplementary online Table 3 (including TMV-MP and TSWV-MP, two well characterized plant virus 30 kDa proteins) were aligned by PROMALS3D and the results are displayed in Supplementary online Fig. 1, limiting the display to the conserved region with parallels beta strands. We observed that using both fungal and plant virus putative MPs, 8 conserved beta sheets are displayed, and the alignment maintained the conserved D residue common to this set of proteins.

The same proteins aligned by PROMALS3D were used to derive alignments by MAFFT and CLUSTAL OMEGA alignment software. Phylogenetic analysis was carried out from PROMALS3D, MAFFT and CLUSTAL OMEGA alignments and the phylogenetic tree showed a clear separation between MP-like proteins in the *Phenuiviridae* and MP proteins from *Aspiviridae*. TSWV-MP and TMV-MP were not associated with any of the two groups with sufficient statistical support (Fig. 2 and Supplementary online Fig. 2).

In summary, protein sequence conservation analysis showed that

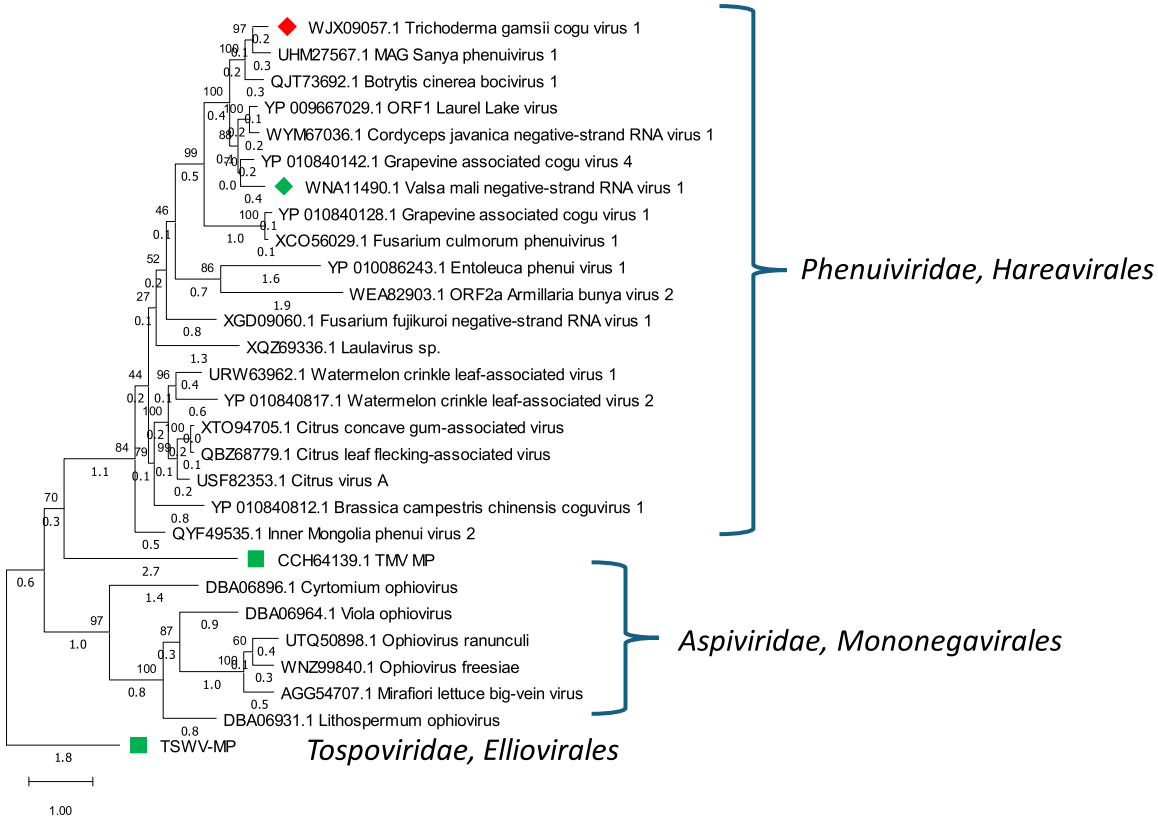

Figure 2. Consensus phylogenetic tree derived from MP and MP-like proteins aligned by MAFFT. Input data: 28 sequences with 399 amino-acid sites; Number of constant sites: 2 (= 0.501253% of all sites); Number of invariant (constant or ambiguous constant) sites: 2 (= 0.501253% of all sites); Number of parsimony informative sites: 391; Number of distinct site patterns: 399. Best-fit model according to BIC: rtREV+F+I+G4. Consensus is constructed from 1000 bootstrap trees. Log-likelihood of consensus tree: -19487.082. Green squares and diamonds are movement proteins (MP) from confirmed plant viruses. A red triangle points to the MP-like proteins focus of this paper. Bootstrap percentages and branch lengths are reported.

homologues of TgCl-MPl proteins are present in some phenuivirid genera, in which VmNSRV1 MP-like protein was recently functionally characterized as MP (Dai et al., 2024), while some very distant relationship can be traced also to MP of the aspivirids.

3.2. Structural analysis

Since protein sequence conservation was not sufficient to strongly support a functional link with plant virus MP, we performed a 3D structural prediction in silico of TgCl-MPl protein with Alphafold3: Fig. 3 panel A and B shows that the predicted structure has regions of high pLDDT (mostly an 8-stranded β-sheet arranged in an antiparallel jelly-roll conformation in the central core of the protein, displayed in panel C) and a few moderately supported α-helices interspersed with connecting loops with much lower pLDDT score. Finally, a few peripheral loops are in a region of high flexibility and disorder.

We then proceeded to search protein structure databases (PDB and those predicted by Alphafold) for similar structures using Foldseek. The PDB search revealed several cryo-EM and X-ray derived structures of viral coat proteins (Supplementary online Table 4). When the BFVD database was interrogated, the results (the first 10 hits are displayed in Supplementary online Table 5) showed that the first hits corresponded to phenuivirids belonging to the *Bocivirus* and *Laulavirus* genera; moreover, some plant virus movement proteins also appeared in the first 15 hits: the MP BC1 of a member of the *Begomovirus* in the *Geminiviridae* (Bean latent virus) and the 30kDa MP protein of the tobamovirus Hibiscus latent Singapore virus. Direct comparison of some closely related predicted structures by matchmaker in ChimeraX confirmed the high conservation of the antiparallel 7/8 β-sheet, which in the case of members of the phenuivirids extends also to other surrounding alpha-helices. The central core spans aa positions 150-296 whereas other conserved alpha-helices are included in a larger fragment spanning aa positions 94-315. We derived structures of phenuivirids representing viruses occupying diverse ecological niches, including some not present in the BFVD dataset (limited to 2023). Specifically, we selected Hibiscus latent Singapore virus and watermelon crinkle leaf-associated virus 2 as examples of true plant viruses, and as a putative insect viruses member of the genus *Horwuvirus* (a possible insect-specific genus inside the *Phenuiviridae*) Solenopsis invicta virus 14 and a virus identified in tick virome studies named Wuhan horsefly horovirus, and therefore unlikely to interact with plants (displayed in Supplementary online Fig. 3). All of them have the conserved single jelly-roll conformation domain, including some of the extended alpha-helices.

3.3. TgClV1-MPl protein subcellular localization

Most plant movement proteins have distinctive subcellular localization: they are enriched at the plasmodesmata and often cause tubule formation of protoplast. In our experiment we included a positive control (pBIN-OuMV-MP-GFP) that was previously extensively studied by our group (Margaria et al., 2016; Ozber et al., 2019). We derived an amino terminal in frame fusion of GFP with TgCl-MPl expressed constitutively under the 35S promoter. As a negative control, we included the same plasmid, but with a stop codon at the end of the GFP,

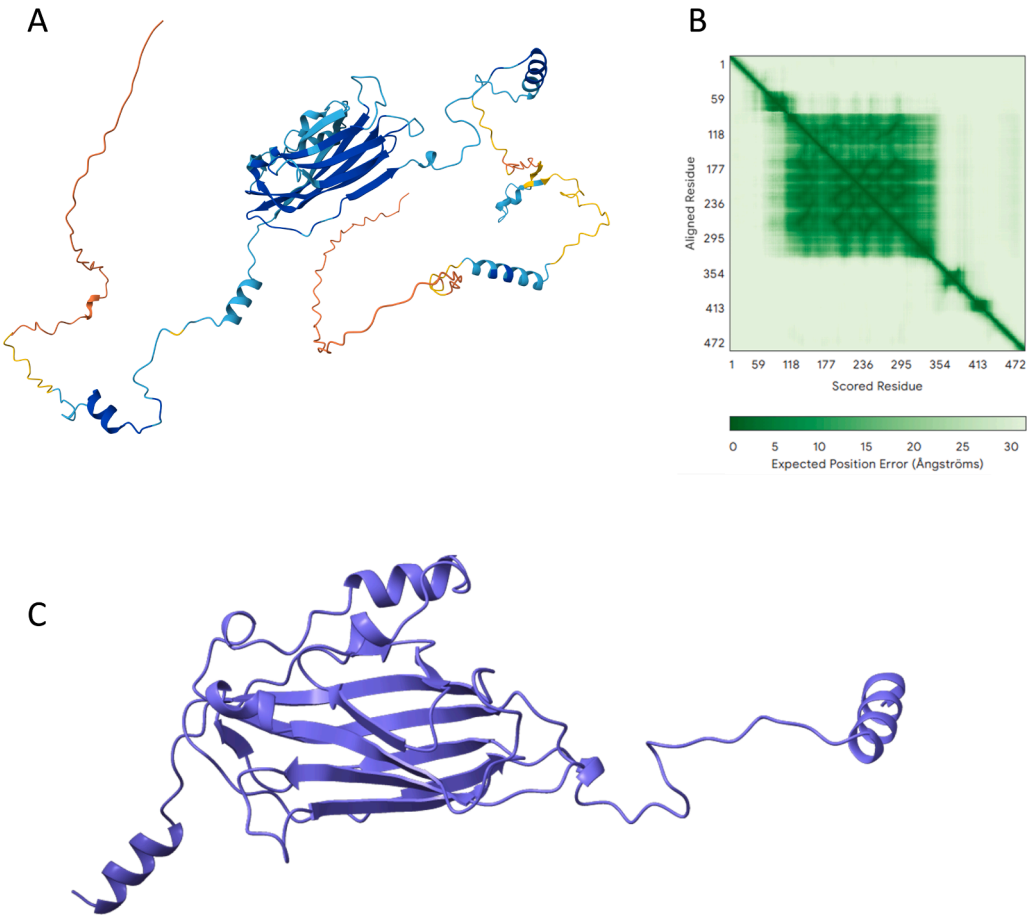

Figure 3. Alphafold 3 prediction of Trichoderma gamsii Cogu-like Virus 1 -MP-like (TgCl-MPl) protein. In panel A The 3D structure of the protein is colored according to the Predicted Local Distance Difference Test (pLDDT) confidence score: dark blue and light blue are for very high and high confidence respectively; yellow and orange are for low and very low confidence respectively. In panel B, a graph representing the expected position errors is also depicted with the main subdomains of high confidence. Panel C is a closeup view of the most conserved part of the protein containing the antiparallel beta-sheets and a few conserved alpha-helices.

that prevents the fusion.

We agroinfiltrated leaves and results are displayed in Fig. 4. The positive MP control shows abundant accumulation of GFP fusion to large compartments close to the cell walls, and some distinctive threads of fluorescence are seen across cell walls.

Regarding our amino terminal GFP-TgCl-MPl fusion construct, to obtain comparable amounts of fluorescence we had to increase laser intensity from 2.5 % (used for the other two constructs) to 10%. The fluorescence was no longer in the nucleus, but we could not provide clear evidence of a cell-wall and plasmodesmata localization. A C-terminal fusion of GFP with MP was barely detectable in leaves, only increasing laser intensity further, but no localization to plasmodesmata was observed (not shown). As a marker of plasmodesmata, we also included a construct expressing PDLP1 fused to GFP: in the same experimental conditions that showed lack of puncta for the GFP-TgCl-MPl fusion, PDLP1 showed concentrated GFP expression in *puncta* at

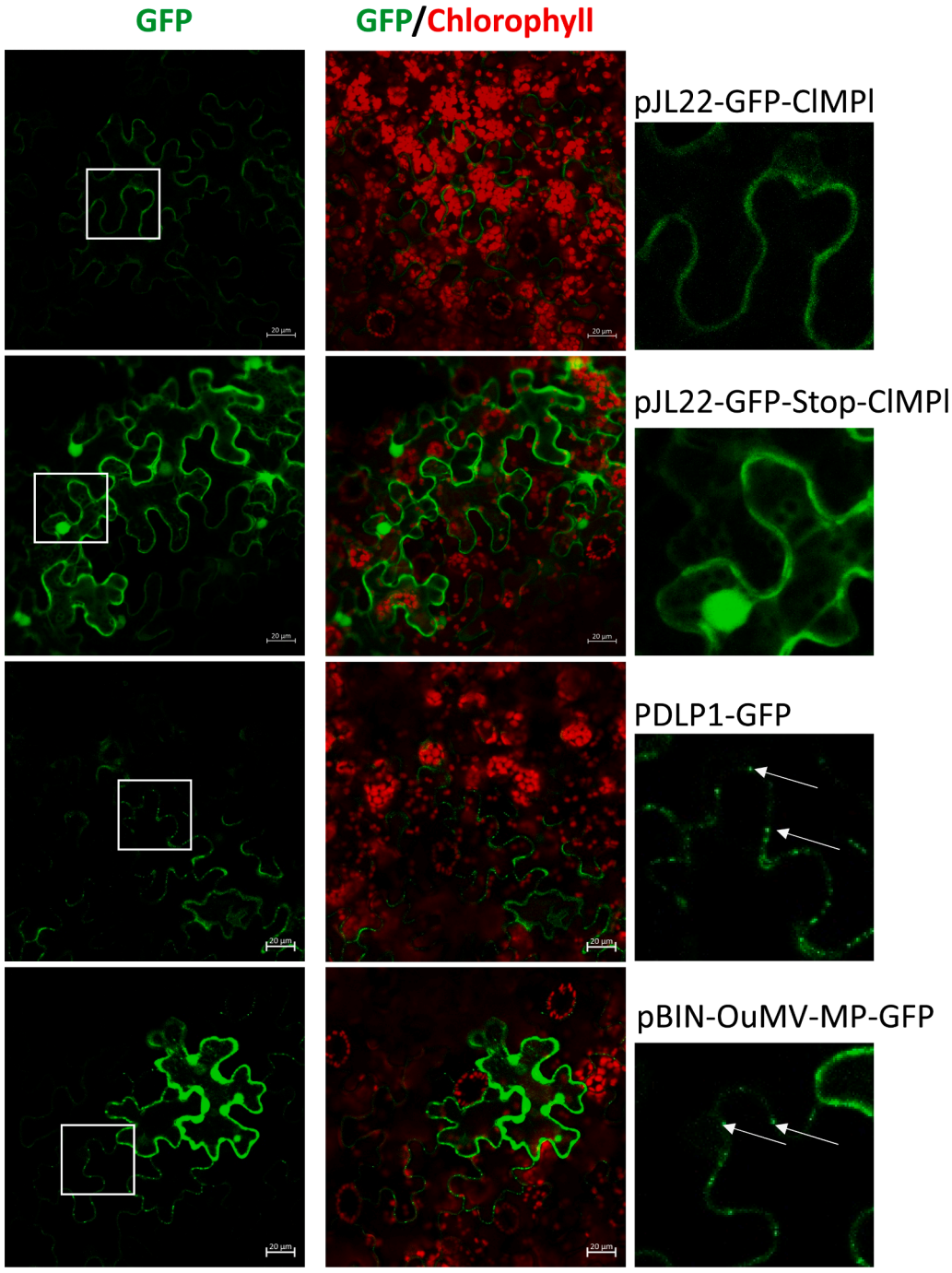

Figure 4. Trichoderma gamsii cogu-like virus 1 encoded MP-like protein (TgCl-MPl) does not localize to plasmodesmata. Confocal microscopy observation of epidermal cells obtained from agroinfiltrated areas was carried out three days post inoculation. Left end panels show acquisition of GFP while the right end panel includes acquisition of chlorophyll auto-fluorescence as a marker of chloroplast organelles. A specific fainter GFP expression is visible for the plasmid expressing Trichoderma gamsii cogu-like virus 1 encoded MP-like protein fused to GFP (pJL22-GFP-ClMPl). The same construct that expresses the only GFP localizes partly to the nucleus (pJL22-GFP-Stop-ClMPl). In the same conditions the two markers for plasmodesmata localization (PDLP1 and OuMV MP, expressed by the construct PDPLP1-GFP and pBIN-OuMV-MP-GFP) have a typical localization as puncta at the cell wall (visible in lower expressing cells in the case of pBIN-OuMV-MP-GFP construct) (white arrows).

the cell walls, as expected by PDLP1 (Thomas et al., 2008) (Fig. 4).

Furthermore, in protoplasts, small protruding fluorescent tubules were readily detected with the ourmiavirus MP-GFP fusion. Our negative control that expresses GFP only, shows accumulation in the nucleus and throughout the cytoplasm. Protoplasts from negative control (GFP only) also showed a sharp edge, without evidence of fluorescent protrusions. Lack of protrusion was also shown for the GFP-TgCl-MPl fusion. (Fig. 5).

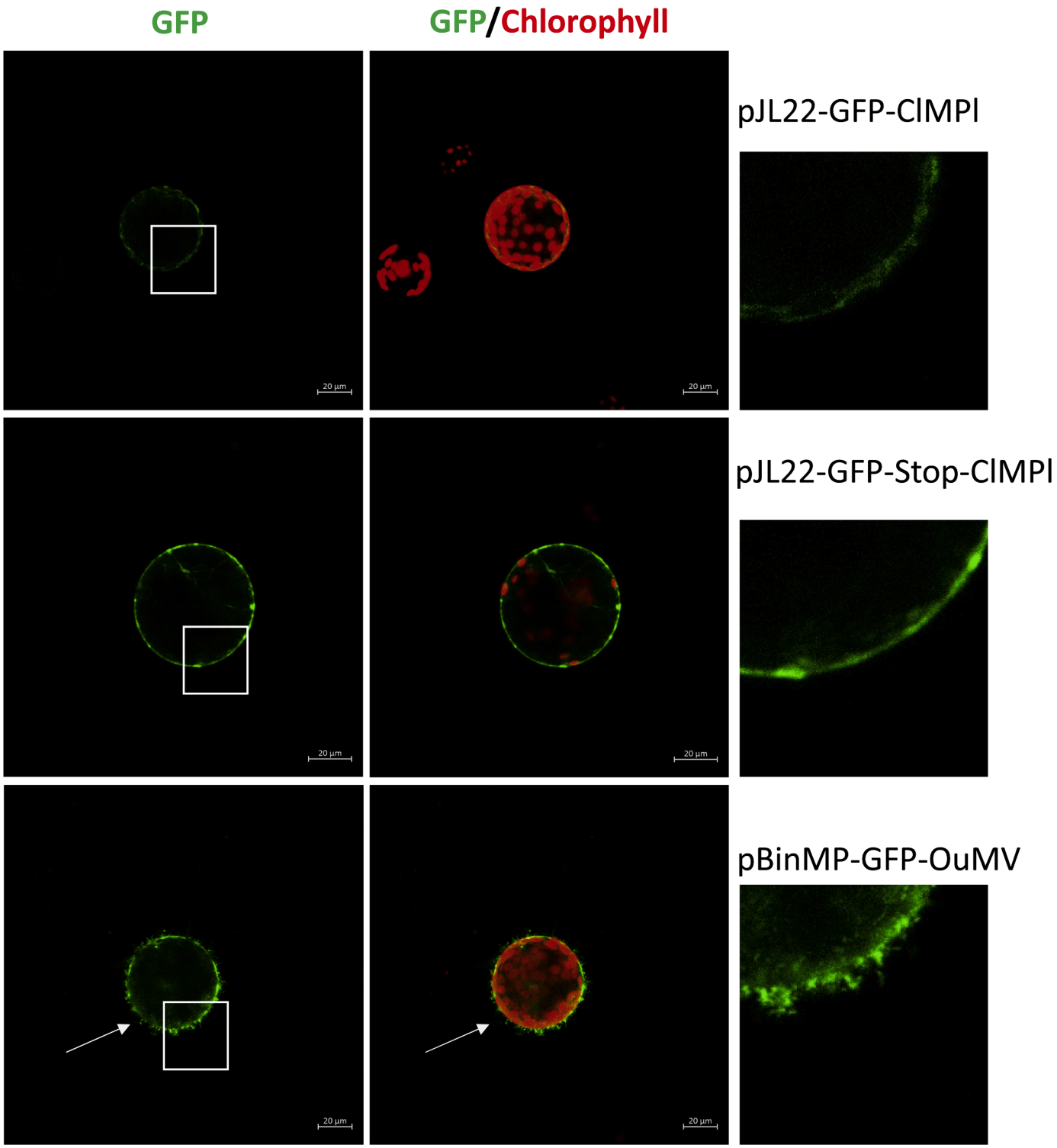

Figure 5. Trichoderma gamsii cogu-like virus 1 encoded MP-like protein (TgCl-MPl) does not form tubules in transfected protoplasts. Confocal microscopy observation of protoplast suspensions obtained from agroinfiltrated areas was carried out three days post inoculation. Tubules surrounding the whole protoplast margin are seen with the MP-GFP fusion from Ourmia melon virus (OuMV) expressed by the plasmid pBinMP-GFP-OuMV (white arrows). No tubules were observed either in the pJL22-GFP-ClMPl or pJL22-GFP-Stop-ClMPl expressing GFP fused to TgCl-MPl and only GFP respectively. Left end panels show acquisition of GFP while the right end panel includes acquisition of chlorophyll auto-fluorescence as a marker of chloroplast organelles. The right end panels are enlargements of the section inside the white square.

3.4. Functional complementation

The ToANV MP deletion GFP-expressing vector has never been used as a virus to be complemented in trans by expression of putative MP. Here we show that a 1:625 dilution results in single-cell infections if an empty vector is co-expressed at saturating concentration (Fig. 6-A). When TMV-MP is expressed at saturating concentration, clusters of cells are visible already 3 dpi (Fig. 6-A). Such clusters enlarge at 5 dpi (not

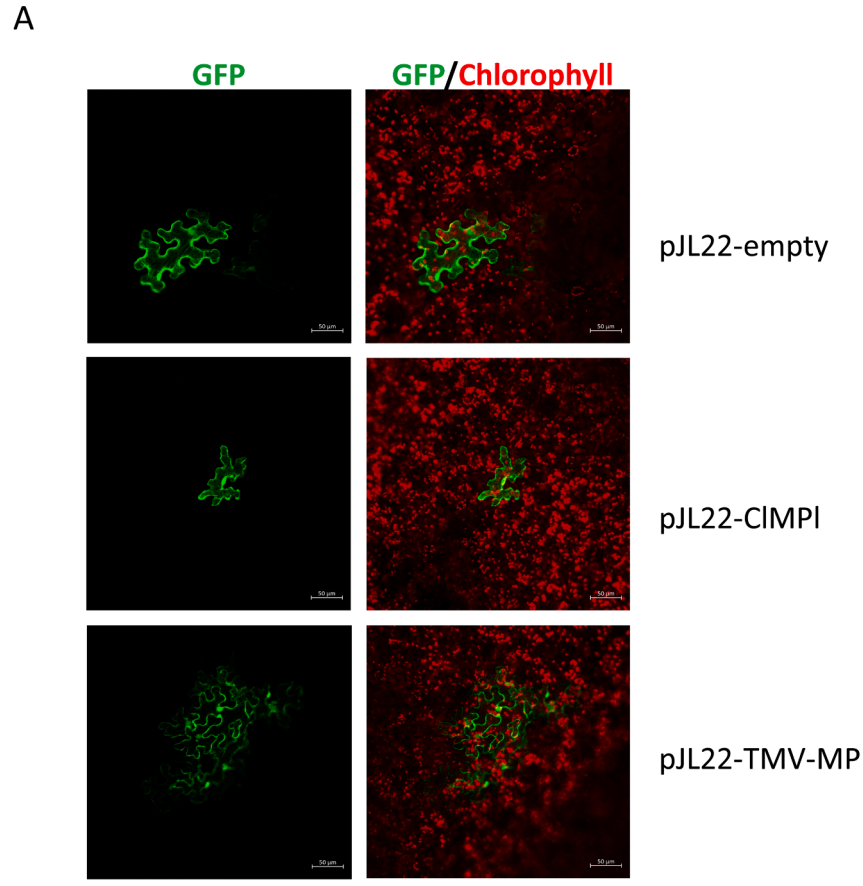

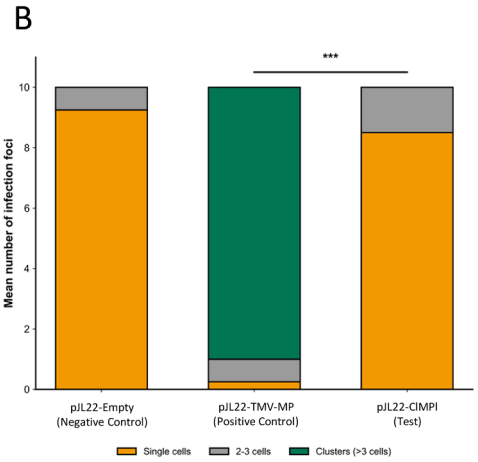

C

Treatment	Type	Clusters (Mean ± SEM)	vs pJL22-TMV-MP	vs pJL22-Empty
pJL22-Empty	Negative Control	0.00 ± 0.00	P <0.001 ***	-
pJL22-TMV-MP	Positive Control	9.00 ± 0.00	-	P <0.001 ***
pJL22-ClMPl	Test	0.00 ± 0.00	P <0.001 ***	P = 1.0000 NS

Figure 6. Trichoderma gamsii cogu-like virus 1 encoded MP-like protein (TgCl-MPl) does not complement tomato apex necrosis (ToANV) movement protein (MP) deficient vector. Panel A: Confocal observation of epidermal cells agroinfiltrated with tomato apex necrosis virus GFP expressing movement-deficient vector. Observation was carried out 3 days post agroinfiltration. The left end panels display GFP fluorescence, while the central panels include acquisition of chlorphyll auto-fluorescence as a marker of chloroplast organelles. The vector-expressing Agrobacterium suspension was diluted serially until distant single cells infection are seen in the negative control (pJL22-empty). The positive control construct pJL22-TMV-MP complemented movement to form small clusters of infected cells, while the TgCl-MPl-expressing construct (pJL22-ClMPl) was indistinguishable from the negative control. Panel B: distribution of infection foci by size category (single cells, 2-3 cells, or clusters >3 cells) for negative control (JL22-Empty), positive control (pJL22-TMV-MP), and test construct (pJL22-ClMPl). Cluster formation indicates successful complementation of viral cell-to-cell movement. Bars represent mean values from four biological replicates. Panel C: Statistical summary showing mean cluster formation ± SEM and pairwise comparison P-values. Statistical significance was determined by Kruskal-Wallis test ($H = 10.67$, $P = 0.0048$) followed by Mann-Whitney U tests with Bonferroni correction ($\alpha = 0.0167$). *** $P < 0.001$; NS, not significant ($P > 0.05$); dash (-) indicates reference group. $n = 4$ biological replicates per treatment.

shown). When TgCl-MPl protein is expressed by agroinfilatration at saturating concentration, there are no clusters formed (Fig. 6, panel A). Quantitative assessment is displayed in Supplementary on line Table 6 and in Fig. 6 panel B and C.

The same results were obtained using a PVX GFP expressing vector with a deletion in the p25 protein of the triple gene block (involved in viral cell to cell movement), the system that was indeed used to prove that VmNSRV1-MP was functional (Dai et al, 2024); our results displayed in Supplementary on line Fig. 4 show that the TgCl-MPl protein does not complement movement. Detailed measurements are displayed in Supplementary Table 7 and Supplementary online Fig. 4 panel B and C, with appropriate statistical treatment.

Finally, TgCl-MPl, when tested in the AMV system which had previously been shown to be complemented by a vast array of putative MP, also failed to complement movement (Supplementary online Fig. 5).

3.5. Plant infectivity assay

Virus purification resulted in the concentration of viral RNA in the pellet of a high-speed centrifugation; observation at the electron microscopy did not reveal any obvious nucleocapsid particle. The purified material used for mechanical rub-inoculation of *N. benthamiana* or leaf infiltration did not result in systemic infection (Supplementary online Fig. 6 and Supplementary online Table 8).

Likewise, tomato plants (*Solanum lycopersicum*) with roots closely associated with mycelia of the CgClV1-infected strain 2226 (inferred by a specific qRT-PCR for viral segment RNA3) did not result in systemic infection with CgClV1 (RT-qPCR Supplementary table) (Supplementary on line Fig. 6 and Supplementary online table 8).

4. Discussion

This study demonstrates that TgCl-MPl, despite containing the conserved single jelly-roll domain characteristic of the 30 kDa movement protein superfamily, does not function as a plant viral movement protein. Three independent lines of evidence support this conclusion: (i) TgCl-MPl failed to complement movement-deficient vectors in three different plant virus systems (ToANV, PVX, AMV), while TMV-MP successfully complemented all three; (ii) unlike functional MPs, TgCl-MPl did not localize to plasmodesmata or form tubules in protoplasts; and (iii) neither mechanical inoculation nor fungal-mediated delivery of TgClV1 resulted in plant infection. These findings contrast with recent reports that VmNSRV1, a related phenuivirid, encodes a functional MP and naturally infects both fungal and plant hosts (Dai et al., 2024), raising important questions about the evolution of cross-kingdom infectivity in mycoviruses.

Plant viral MP studies are arguably among the best examples of how studying virus molecular biology has helped elucidating basic biological aspects of their host: the discovery of the universal presence in plant viruses of genes that facilitate their movement through plasmodesmata began with the discovery and characterization of TMV MP, the first member of a family of proteins widespread in plant viruses, the 30 kDa (DEOM et al., 1987; MESHI et al., 1987) . This discovery led later to the discovery of “functional paralogues” of plant movement proteins, such as KNOTTED1 and CmPP16: these were seminal discoveries in elucidating mechanistically the existence of non-cell-autonomous proteins in plants (NCAPs) showing that indeed plasmodesmata can be specifically gated for long distance movement of proteins or RNA-protein complexes (LUCAS et al., 1995; Xoconostle-Cázares et al., 1999).

While movement of virus within a plant individual has received a wealth of ongoing in depth studies, conversely, movement of viruses inside fungal individuals has not received a proper experimental confirmation of the common assumption that mycovirus flow freely in the cytoplasm: ancient fungi are coenocytic, while ascomycetes and basidiomycetes do indeed have septa that separates cells, but the assumption is that the selective pressure on trafficking among plant cells imposed by plasmodesmata is not mimicked by septa in fungi, which instead allows free-flow of proteins, RNA and organelles often referred to as “open permeability” (Bleichrodt et al., 2015; Steinberg et al., 2018; Wang and Dean, 2020). In fact, mycoviruses do not encode proteins facilitating movement in the hyphae and some mycoviruses have very simple genome organizations and the only common function attribution to mycoviruses encoded protein is cell-autonomous genome replication.

As mentioned in the introduction, several fungal viruses have close relative as “cryptic” plant viruses (Takahashi et al., 2019) suggesting a trans-kingdom evolutionary trajectory likely going from fungi to plants (a small number of plant virus are embedded in wider mycovirus clades), but up until recently, the specific lifestyle of these viruses indicated that they can not move from cell to cell in plants, and maintain infections because they can infect meristematic tissues, and are transmitted vertically through seeds and pollens. Noticeably these viruses cannot be mechanically transmitted, a hallmark of inability to move from cell to cell in plants.

Recently, however, two confirmed mycoviruses have been shown to be able to also infect plants: in one case, a new circular single-stranded DNA mycovirus named Diaporthe sojae circular DNA virus 1 (DsCDV1) encodes for a functional plant MP and can infect mechanically tobacco and pear trees, and in this case, the functional MP (P3) is not conserved with any known plant virus MP (Wang et al., 2024); this virus is the type virus of a new proposed family named “Gegemycoviridae”.

In the second case, a phenuivirid was convincingly shown to encode a plant MP: the VmNSRV1 RNA2-encoded protein localizes to plasmodesmata and can complement a p25 triple gene block protein knock out mutant of PVX. In elegant experiments, the authors showed that the phytopathogenic fungus *Valsa mali* can acquire the virus from apple plants, and *V. mali* infection is less symptomatic on apple plants carrying the cryptic virus infection, showing a biotechnological potential of this cross-kingdom infection event. The protein encoded by VmNSRV1 RNA2 indeed displays the single jelly roll motif which seems to be common to the 30 kDa family of MP (Dai et al., 2024).

In our case, we could not confirm that a homologue of VmNSRV1 MP has the same function suggesting that the single jelly-roll structure might be involved in processes other than those related to plant infection or virion formation (we can exclude a structural role of MP-like proteins since these entire class of viruses encodes for a proper nucleocapsid protein).

Our results raise a critical evolutionary question: does TgClV1 represent loss-of-function from a plant-infecting ancestor, or does VmNSRV1 represent recent gain-of-function for plant adaptation? Several lines of evidence suggest VmNSRV1 could be the exception. In this regard, it is worth noting that the MP-like proteins encoded by genera of plant virus and mycovirus inside the phenuivirids have not been functionally characterized even in the case of putative *bona fidae* plant viruses, like those belonging to the genus *Coguvirus*: indeed, coguviruses are not easily mechanically transmitted and in most case they are maintained through grafting (Navarro et al., 2018; Xin et al., 2017).

Furthermore, caution should be exercised when considering the single jelly-roll structure as a hallmark of plant MPs. In phenuivirids, this structural fold is also present in the genus Horwuvirus (Supplementary online Fig. 3), which appears to be enriched in bona fide insect viruses whose hosts show no apparent association with plants. For example, Fitzroy Crossing tenui-like virus 1 h was associated to mosquitoes of the genus Culex, which do not establish close biological interactions with plants (Williams et al., 2020). Another member of the genus (Solenopsis invicta virus 14) that encodes a MP-like protein, was found in studies of the virome associated with fire ants (*Solenopsis invicta*): based on different in silico approaches, the authors suggest that indeed this is an insect virus, which would raise the question of the role of the MP-like protein present in its genome: do fire ants transmit a plant virus? Or, more likely a fungus is involved and MP-like proteins have other functions (i.e. the single jelly-roll domain was exapted for other purposes

than plasmodesmata gating); the possible involvement of a fungus is a hypothesis not taken in consideration by the authors (Xavier et al., 2021), but it could explain some erratic tropism observed in their studies. Another virus belonging to *Laulavirus* genus (the same genus that includes VmNSRV1), Lurel Lake Virus, was found in a black-legged tick, an obligate blood-feeding ectoparasite: nevertheless, the authors themselves suggest that this is a mycovirus infecting the entomopathogenic fungus *Cordyceps brogniartii* (Tokarz et al., 2018; Tokarz et al., 2019). In this case, a relationship with plants is conceivable, since some members of the *Cordyceps* genus were experimentally shown to be plant endophytic fungi (Qiao et al., 2024). Therefore, the presence of a plant MP-like protein in a tick-associated virus may indicate a possible, albeit tenuous, link to plants as an alternative host that remains to be identified. Moreover, another laulavirus was identified in the virome associated to black Flies (De Coninck et al., 2025), which again could support a role different from plant MP for the MP-like protein encoded by this virus.

Interestingly, one of the phenuivirid included in a clade of mycoviruses (still taxonomically not defined but very closely related to genera carrying the MP-like homologues the RNA2) codes for a protein that is likely a glycoprotein, suggesting a new adaptive evolutionary cross-kingdom trajectory from fungi to insect without retaining the single jelly roll structural domain in its sequence (Huang et al., 2023).

What, then, is the actual function of the single jelly-roll domain in plant MP? One could speculate that PD localization is part of the conserved domain, and indeed studies on TMV demonstrate that the PD localization signal, both necessary and sufficient to re-locate fused proteins is partly included in the eight antiparallel β-strands that characterize the single jelly-roll domain present in MP: in fact the PD localization signal (s) correspond to the region 1-50 with AA in position 4 and 14 significantly impacting localization (Yuan et al., 2016) and recent findings demonstrate the presence of two more PD localization signals (AA 61-80 and AA 147-170) (Liu et al., 2020) that are indeed included in the jelly-roll domain that in TMV spans AA 30-180 (Supplementary online Fig. 1); in TMV-MP, the single jelly-roll domain is also the region where RNA binding occurs (AA 50-126 in specific) and the domain required for PD SEL modification (126-185); while the first part of the domain seems to possibly adapted to a number of different functions that include interaction with RNA, the second part of the domain seem to be more related to plant movement.

We acknowledge two limitations in definitively excluding plant-infection capacity for TgClV1. First, we have not identified TgClV1′s natural plant host (if one exists), which might have specific cellular requirements not met by our experimental hosts (*N. benthamiana* and *S. lycopersicum*). In this respect we also did not test if the virus itself can replicate in plant cells, a prerequisite to be a plant virus. Second, successful trans-complementation can be virus-family-specific; however, this concern is mitigated by testing three phylogenetically diverse systems and by the fact that TMV-MP successfully complemented all three.

Despite these caveats, the convergence of multiple negative results—failed complementation in three systems, absent PD localization, lack of tubule formation, and failed plant infection—strongly supports our conclusion that TgCl-MPl does not function as a plant MP under standard conditions.

In this sense it is worth reminding of the dual ecological nature of *T. gamsii*, the natural host of TgClV1: like many *Trichoderma* species, *T. gamsii* is a soil-dwelling saprotroph with high rhizosphere competence that frequently forms beneficial plant associations, including endophytic colonization (Contreras-Cornejo et al., 2016; Rinu et al., 2014; Zhou et al., 2018); propensity to endophytic colonization is often strain-specific.

A more general take-home message of our work also calls for caution in ORF annotations simply based on sequence or structural conservation, as with the case of the likely incorrect MP annotation of an ORF present in members of the family *Tobaliviridae* (Sabanadzovic et al., 2026).

Finally, while many mycoviruses were thought to have a simple genomic organization, after untargeted HTS approaches more and more multisegmented genomes were found coding for proteins with unknown functions (for example the narnavirus-like clade exemplifies this shift in complexity): this could imply that a number of still unknown complex intra- and inter-organism processes are to be discovered as a driver for virus evolution in fungi. In specific, a reverse genetic system for fungus-infecting phenuivirids would allow to elucidate the role of MP-like knock outs on virus fitness in fungal hosts.

Funding

This study was supported by the Next Generation EU PRIN 2022: "MYCOVIROLE: Viromes of fungi interacting with plants: roles in adaptation to different/extreme ecological niches and reservoir of viral biodiversity for potential spillover" (20222L5ECJ, CUP B53D23011710006).

CRediT authorship contribution statement

Federica Bono: Writing – review & editing, Visualization, Methodology, Investigation. **Ian Martinelli:** Writing – review & editing, Methodology, Investigation. **Yi Guo:** Writing – review & editing, Visualization, Investigation. **Saul Pagnoni:** Writing – review & editing, Visualization, Methodology, Investigation, Conceptualization. **Frederic Aparicio Herrero:** Writing – review & editing, Visualization, Investigation. **Massimo Turina:** Writing – review & editing, Writing – original draft, Methodology, Investigation, Funding acquisition, Formal analysis, Conceptualization.

Declaration of competing interest

The authors declare no competing financial or personal interests that could have appeared to influence the work reported in this paper.

Supplementary materials

Supplementary material associated with this article can be found, in the online version, at doi:10.1016/j.virusres.2026.199741.

Data availability

The data is shared in supplementary tables included in the material available to the readers

References

Abramson, J., Adler, J., Dunger, J., Evans, R., Green, T., Pritzel, A., Ronneberger, O., Willmore, L., Ballard, A., Bambrick, J., Bodenstein, S., Evans, D., Hung, C., O'Neill, M., Reiman, D., Tunyasuvunakool, K., Wu, Z., Zemgulyte, A., Arvaniti, E., Beattie, C., Bertolli, O., Bridgland, A., Cherepanov, A., Congreve, M., Cowen-Rivers, A., Cowie, A., Figurnov, M., Fuchs, F., Gladman, H., Jain, R., Khan, Y., Low, C., Perlin, K., Potapenko, A., Savy, P., Singh, S., Stecula, A., Thillaisundaram, A., Tong, C., Yakneen, S., Zhong, E., Zielinski, M., Zídek, A., Bapst, V., Kohli, P., Jaderberg, M., Hassabis, D., Jumper, J., 2024. Accurate structure prediction of biomolecular interactions with AlphaFold 3 (vol 630, pg 493, 2024). Nature 636 (8042), E4.

Andika, I.B., Wei, S., Cao, C., Salaipeth, L., Kondo, H., Sun, L., 2017. Phytopathogenic fungus hosts a plant virus: a naturally occurring cross-kingdom viral infection. Proc. Natl. Acad. Sci. 114 (46), 12267–12272.

Bleichrodt, R., Hulsman, M., Wösten, H., Reinders, M., 2015. Switching from a unicellular to multicellular organization in an *Aspergillus niger* Hypha. Mbio 6 (2).

Butkovic, A., Dolja, V.V., Koonin, E.V., Krupovic, M., 2023. Plant virus movement proteins originated from jelly-roll capsid proteins. PLoS Biol. 21 (6), e3002157.

Chiapello, M., Bosco, L., Ciuffo, M., Ottati, S., Salem, N., Rosa, C., Tavella, L., Turina, M., 2021. Complexity and local specificity of the virome associated with tospovirus-transmitting thrips species. J. Virol. 95 (21).

Contreras-Cornejo, H., Macías-Rodríguez, L., del-Val, E., Larsen, J., 2016. Ecological functions of *trichoderma* spp. And their secondary metabolites in the rhizosphere: interactions with plants. Fems Microbiol. Ecol. 92 (4).

Dai, R., Yang, S., Pang, T., Tian, M., Wang, H., Zhang, D., Wu, Y., Kondo, H., Andika, I., Kang, Z., Sun, L., 2024. Identification of a negative- strand RNA virus with natural plant and fungal hosts. Proc. Natl. Acad. Sci. U. S. A. 121 (12).

De Coninck, L., Hadermann, A., Ingletto, L., Colebunders, R., Njamnshi, K., Njamnshi, A., Mokili, J., Fodjo, J., Matthijnssens, J., 2025. Cameroonian blackflies (Diptera: Simuliidae) harbour a plethora of RNA viruses. Virus Evol. 11 (1).
Deom, C., Oliver, M., Beachy, R., 1987. The 30-kilodalton gene-product of tobacco mosaic-virus potentiates virus movement. Science 237 (4813), 389–394.
Diep Thi, H., Chernomor, O., von Haeseler, A., Minh, B.Q., Le Sy, V., 2018. UFBoot2: Improving the Ultrafast bootstrap approximation. Mol. Biol. Evol. 35 (2), 518–522.
Dorokhov, Y.L., Sheshukova, E.V., Byalik, T.E., Komarova, T.V., 2020. Diversity of plant virus movement proteins: what do they have in common? Processes 8 (12).
Ferriol, I., Turina, M., Zamora-Macorra, E.J., Falk, B.W., 2016. RNA1-Independent replication and GFP expression from Tomato marchitez virus isolate M cloned cDNA. Phytopathology 106 (5), 500–509.
Ferriol, I., Vallino, M., Ciuffo, M., Nigg, J.C., Zamora-Macorra, E.J., Falk, B.W., Turina, M., 2018. The torradovirus-specific RNA2-ORF1 protein is necessary for plant systemic infection. Mol. Plant Pathol. 19 (6), 1319–1331.
Forgia, M., Daghino, S., Chiapello, M., Ciuffo, M., Turina, M., 2024. New clades of viruses infecting the obligatory biotroph bremia lactucae representing distinct evolutionary trajectory for viruses infecting oomycetes. Virus Evol. 10 (1).
Heinlein, M., 2015a. Plant virus replication and movement. Virology 479, 657–671.
Heinlein, M., 2015b. Plasmodesmata: channels for viruses on the move. Plasmodesmata: Methods Protoc. 1217, 25–52.
Huang, H., Hua, X.M., Pang, X.D., Zhang, Z.M., Ren, J.Y., Cheng, J.S., Fu, Y.P., Xiao, X. Q., Lin, Y., Chen, T., Li, B., Liu, H.Q., Jiang, D.H., Xie, J.T., 2023. Discovery and characterization of putative glycoprotein-encoding mycoviruses in the *Bunyavirales*. J. Virol. 97 (1).
Janda, M., Ahlquist, P., 1993. Rna-dependent replication, transcription, and persistence of brome mosaic-virus Rna replicons In saccharomyces-cerevisiae. Cell 72 (6), 961–970.
Kalyaanamoorthy, S., Bui Quang, M., Wong, T.K.F., von Haeseler, A., Jermiin, L.S., 2017. ModelFinder: fast model selection for accurate phylogenetic estimates. Nat. Methods 14 (6), 587. -+.
Katoh, K., Rozewicki, J., Yamada, K.D., 2019. MAFFT online service: multiple sequence alignment, interactive sequence choice and visualization. Brief. Bioinform. 20 (4), 1160–1166.
Kim, R., Karin, E., Mirdita, M., Chikhi, R., Steinegger, M., 2024. BFVD-a large repository of predicted viral protein structures. Nucleic Acids Res. 53 (D1), D340–D347.
Kuhn, J., Brown, K., Adkins, S., de la Torre, J., Digiaro, M., Ergünay, K., Firth, A., Hughes, H., Junglen, S., Lambert, A., Maes, P., Marklewitz, M., Palacios, G., Sasaya, T., Shi, M., Zhang, Y., Wolf, Y., Turina, M., 2024. Promotion of order *Bunyavirales* to class *Bunyaviricetes* to accommodate a rapidly increasing number of related polyploviricotine viruses. J. Virol. 98 (10), e01069. -24.
Kumar, S., Stecher, G., Suleski, M., Sanderford, M., Sharma, S., Tamura, K., 2024. MEGA12: Molecular Evolutionary Genetic Analysis Version 12 for adaptive and green computing. Mol. Biol. Evol. 41 (12).
Lam-Tung, N., Schmidt, H.A., von Haeseler, A., Bui Quang, M., 2015. IQ-TREE: A fast and effective stochastic algorithm for estimating maximum-likelihood phylogenies. Mol. Biol. Evol. 32 (1), 268–274.
Lindbo, J.A., 2007. High-efficiency protein expression in plants from agroinfection-compatible tobacco mosaic virus expression vectors. Bmc Biotechnol. 7.
Liu, Y., Huang, C., Zeng, J., Yu, H., Li, Y., Yuan, C., 2020. Identification of two additional plasmodesmata localization domains in the tobacco mosaic virus cell-to-cell-movement protein. Biochem. Biophys. Res. Commun. 521 (1), 145–151.
Liu, Z., Kearney, C.M., 2010. An efficient Foxtail mosaic virus vector system with reduced environmental risk. Bmc Biotechnol. 10.
Lucas, W., Bouchepillon, S., Jackson, D., Nguyen, L., Baker, L., Ding, B., Hake, S., 1995. Selective trafficking of Knotted1 homeodomain protein and its messenger-Rna through plasmodesmata. Science 270 (5244), 1980–1983.
Madeira, F., Madhusoodanan, N., Lee, J., Eusebi, A., Niewielska, A., Tivey, A., Lopez, R., Butcher, S., 2024. The EMBL-EBI Job Dispatcher sequence analysis tools framework in 2024. Nucleic Acids Res. 52 (W1), W521–W525.
Margaria, P., Anderson, C.T., Turina, M., Rosa, C., 2015. Identification of an ourmiavirus 30K movement protein amino acid residues involved in symptomatology, viral movement, subcellular localization and tubule formation. Mol. plant pathol. 17 (7), 1063–1079.
Margaria, P., Anderson, C.T., Turina, M., Rosa, C., 2016. Identification of Ourmiavirus 30K movement protein amino acid residues involved in symptomatology, viral movement, subcellular localization and tubule formation. Mol. Plant Pathol. 17 (7), 1063–1079.
Margaria, P., Turina, M., Palmano, S., 2009. Detection of flavescence doree and Bois noir phytoplasmas, Grapevine leafroll associated virus-1 and -3 and Grapevine virus A from the same crude extract by reverse transcription-RealTime Taqman assays. Plant Pathol. 58 (5), 838–845.
Meshi, T., Watanabe, Y., Saito, T., Sugimoto, A., Maeda, T., Okada, Y., 1987. Function of the 30-kd protein of tobacco mosaic-virus - involvement In cell-to-cell movement and dispensability for replication. Embo J. 6 (9), 2557–2563.
Migheli, Q., Balmas, V., Komon-Zelazowska, M., Scherm, B., Fiori, S., Kopchinskiy, A.G., Kubicek, C.P., Druzhinina, I.S., 2009. Soils of a Mediterranean hot spot of biodiversity and endemism (Sardinia, Tyrrhenian Islands) are inhabited by pan-European, invasive species of Hypocrea/Trichoderma. Environ. Microbiol. 11 (1), 35–46.
Navarro, B., Minutolo, M., De Stradis, A., Palmisano, F., Alioto, D., Di Serio, F., 2018. The first phlebo-like virus infecting plants: a case study on the adaptation of negative-stranded RNA viruses to new hosts. Mol. Plant Pathol. 19 (5), 1075–1089.
Nerva, L., Varese, G.C., Falk, B.W., Turina, M., 2017. Mycoviruses of an endophytic fungus can replicate in plant cells: evolutionary implications. Sci. Rep. 7.
Nerva, L., Vigani, G., Di Silvestre, D., Ciuffo, M., Forgia, M., Chitarra, W., Turina, M., 2019. Biological and molecular characterization of Chenopodium quinoa mitovirus 1 reveals a distinct sRNA response compared to cytoplasmic RNA viruses. J. Virol. 93 (7), 10–1128.
Ozber, N., Margaria, P., Anderson, C., Turina, M., Rosa, C., 2019. Identification of host factors interacting with the movement protein of Ourmia melon virus in Arabidopsis. Phytopathology 109 (10), 187.
Pagnoni, S., Oufensou, S., Balmas, V., Bulgari, D., Gobbi, E., Forgia, M., Migheli, Q., Turina, M., 2023. A collection of trichoderma isolates from natural environments in Sardinia reveals a complex virome that includes negative-sense fungal viruses with unprecedented genome organizations. Virus Evol. 9 (2).
Pei, J.M., Grishin, N.V., 2014. PROMALS3D: multiple protein sequence alignment enhanced with evolutionary and three-dimensional structural information. in: Russell, D.J. (Ed.). Mult. Seq. Alignment Methods 1079, 263–271.
Pettersen, E.F., Goddard, T.D., Huang, C.R.C., Meng, E.E.C., Couch, G.S., Croll, T.I., Morris, J.H., Ferrin, T.E., 2021. UCSF ChimeraX: structure visualization for researchers, educators, and developers. Protein Sci. 30 (1), 70–82.
Qiao, L., Liu, J., Zhou, Z., Li, Z., Zhou, Y., Xu, S., Yang, Z., Qu, J., Zou, X., 2024. Positive effects of *Cordyceps cateniannulata* colonization in tobacco: growth promotion and resistance to abiotic stress (14, 1131184, 2023). Front. Microbiol. 15.
Rinu, K., Sati, P., Pandey, A., 2014. *Trichoderma gamsii* (NFCCI 2177): a newly isolated endophytic, psychrotolerant, plant growth promoting, and antagonistic fungal strain. J. Basic Microbiol. 54 (5), 408–417.
Ruiz-Padilla, A., Rodriguez-Romero, J., Gomez-Cid, I., Pacifico, D., Ayllon, M.A., 2021. Novel mycoviruses discovered in the mycovirome of a necrotrophic fungus. Mbio 12 (3).
Sabanadzovic, S., Aboughanem-Sabanadzovic, N., Turina, M., Suzuki, N., Krupovic, M., 2026. Tobaliviridae", a new family of filamentous mycoviruses in the order *Martellivirales*. Arch. Virol. 171 (2).
Sanchez-Navarro, J., Miglino, R., Ragozzino, A., Bol, J., 2001. Engineering of *Alfalfa mosaic virus* RNA 3 into an expression vector. Arch. Virol. 146 (5), 923–939.
Sasaya, T., Palacios, G., Briese, T., Di Serio, F., Groschup, M., Neriya, Y., Song, J., Tomitaka, Y., 2023. ICTV virus taxonomy profile: *phenuiviridae* 2023. J. Gen. Virol. 104 (9).
Shi, M., Lin, X.-D., Tian, J.-H., Chen, L.-J., Chen, X., Li, C.-X., Qin, X.-C., Li, J., Cao, J.-P., Eden, J.-S., Buchmann, J., Wang, W., Xu, J., Holmes, E.C., Zhang, Y.-Z., 2016. Redefining the invertebrate RNA virosphere. Nature 540 (7634), 539–543.
Sievers, F., Wilm, A., Dineen, D., Gibson, T.J., Karplus, K., Li, W., Lopez, R., McWilliam, H., Remmert, M., Soeding, J., Thompson, J.D., Higgins, D.G., 2011. Fast, scalable generation of high-quality protein multiple sequence alignments using Clustal Omega. Mol. Syst. Biol. 7.
Steinberg, G., Peñalva, M., Riquelme, M., Wösten, H., Harris, S., Heitman, J., Howlett, B., Crous, P., Stukenbrock, E., James, T., Gow, N., 2018. Cell biology of hyphal growth. Fungal Kingdom, 231-265.
Sun, L., Andika, I., Kondo, H., Chen, J., 2013. Identification of the amino acid residues and domains in the cysteine-rich protein of Chinese wheat mosaic virus that are important for RNA silencing suppression and subcellular localization. Mol. Plant Pathol. 14 (3), 265–278.
Sánchez-Navarro, J., Bol, J., 2001. Role of the Alfalfa mosaic virus movement protein and coat protein in virus transport. Mol. Plant-Microbe Interact. 14 (9), 1051–1062.
Sánchez-Navarro, J., Herranz, M., Pallás, V., 2006. Cell-to-cell movement of Alfalfa mosaic virus can be mediated by the movement proteins of Ilar-, bromo-, cucumo-, tobamo- and comoviruses and does not require virion formation. Virology 346 (1), 66–73.
Takahashi, H., Fukuhara, T., Kitazawa, H., Kormelink, R., 2019. Virus Latency Impact Plants. Front. Microbiol. 10.
Thomas, C.L., Bayer, E.M., Ritzenthaler, C., Fernandez-Calvino, L., Maule, A.J., 2008. Specific targeting of a plasmodesmal protein affecting cell-to-cell communication. Plos Biol. 6 (1), 180–190.
Tokarz, R., Sameroff, S., Tagliafierro, T., Jain, K., Williams, S.H., Cucura, D.M., Rochlin, I., Monzon, J., Carpi, G., Tufts, D., 2018. Identification of novel viruses in Amblyomma americanum, Dermacentor variabilis, and Ixodes scapularis ticks. Msphere 3 (2), e00614–e00617.
Tokarz, R., Tagliafierro, T., Sameroff, S., Cucura, D., Oleynik, A., Che, X., Jain, K., Lipkin, W., 2019. Microbiome analysis of *ixodes scapularis* ticks from New York and Connecticut. Ticks Tick-Borne Dis. 10 (4), 894–900.
Trifinopoulos, J., Lam-Tung, N., von Haeseler, A., Minh, B.Q., 2016. W-IQ-TREE: a fast online phylogenetic tool for maximum likelihood analysis. Nucleic Acids Res. 44 (W1), W232–W235.
Turina, M., Ciuffo, M., Lenzi, R., Rostagno, L., Mela, L., Derin, E., Palmano, S., 2006. Characterization of four viral species belonging to the family Potyviridae isolated from Ranunculus asiaticus. Phytopathology 96 (6), 560–566.
Turina, M., Ricker, M.D., Lenzi, R., Masenga, V., Ciuffo, M., 2007. A severe disease of tomato in the Culiacan area (Sinaloa, Mexico) is caused by a new picorna-like viral species. Plant Dis. 91 (8), 932–941.
van Kempen, M., Kim, S., Tumescheit, C., Mirdita, M., Lee, J., Gilchrist, C., Soeding, J., Steinegger, M., 2024. Fast and accurate protein structure search with Foldseek. Nat. Biotechnol. 42 (2).
Wang, M., Dean, R., 2020. Movement of small RNAs in and between plants and fungi. Mol. Plant Pathol. 21 (4), 589–601.
Wang, X., Kotta-Loizou, I., Coutts, R., Deng, H., Han, Z., Hong, N., Shafik, K., Wang, L., Guo, Y., Yang, M., Xu, W., Wang, G., 2024. A circular single-stranded DNA mycovirus infects plants and confers broad-spectrum fungal resistance. Mol. Plant 17 (6), 955–971.
Williams, S., Levy, A., Yates, R., Somaweera, N., Neville, P., Nicholson, J., Lindsay, M., Mackenzie, J., Jain, K., Imrie, A., Smith, D., Lipkin, W., 2020. The diversity and

distribution of viruses associated with *Culex annulirostris* mosquitoes from the Kimberley Region of Western Australia. Viruses-Basel 12 (7).
Xavier, C., Allen, M., Whitfield, A., 2021. Ever-increasing viral diversity associated with the red imported fire ant *solenopsis invicta* (Formicidae: Hymenoptera). Virol. J. 18 (1).
Xin, M., Cao, M., Liu, W., Ren, Y., Zhou, X., Wang, X., 2017. Two negative-strand RNA viruses identified in watermelon represent a novel clade in the order bunyavirales. Front. Microbiol. 8.
Xoconostle-Cázares, B., Yu, X., Ruiz-Medrano, R., Wang, H., Monzer, J., Yoo, B., McFarland, K., Franceschi, V., Lucas, W., 1999. Plant paralog to viral movement protein that potentiates transport of mRNA into the phloem. Science 283 (5398), 94–98.
Yuan, C., Lazarowitz, S., Citovsky, V., 2016. Identification of a functional plasmodesmal localization signal in a plant viral. Cell-To-Cell-Mov. Protein. Mbio 7 (1).
Zhou, D., Huang, X., Guo, J., dos-Santos, M., Vivanco, J., 2018. *Trichoderma gamsii* affected herbivore feeding behaviour on *Arabidopsis thaliana* by modifying the leaf metabolome and phytohormones. Microb. Biotechnol. 11 (6), 1195–1206.